A Smoking Gun for Supersymmetry

Howard E. Haber

UC Davis Theory Seminar

7 February 2011

This talk is based on work that appears in:

1. B.C. Allanach, S. Grab and H.E. Haber, "Supersymmetric Monojets at the Large Hadron Collider," JHEP **1101** (2011) 138 [arXiv:1010.4261 [hep-ph]].

2. H.E. Haber and J.D. Mason, "Hard supersymmetry-breaking 'wrong-Higgs' couplings of the MSSM," *Phys. Rev.* **D77** (2008) 115011 [arXiv:0711.2890 [hep-ph]].

Outline

- Introduction—telltale signs of supersymmetry (SUSY)

  – Significance of the gaugino–particle–sparticle couplings

- Expectations for the lightest supersymmetric particle (LSP)

- Monojets at the LHC: a signal for new physics beyond the Standard Model?

- A proposal to measure the $q\widetilde{q}\widetilde{\chi}_1^0$ coupling

- Gaugino–higgsino–Higgs boson couplings of the MSSM

- Conclusions and future directions

# Introduction—telltale signs of SUSY

Suppose that new physics beyond the Standard Model (SM) is discovered at the LHC. How will we know it is SUSY (taking into account that SUSY is a broken symmetry)?

- Every SM particle has a superpartner differing in spin by half a unit.
  - You may only discover a subset of all the superpartners
  - Spin measurements may be difficult in some cases

- The total number of bosonic and fermionic degrees of freedom must be equal
 - It is very unlikely that all MSSM degrees of freedom can be accessed at the LHC

Perhaps the "gluino" that was discovered is an ordinary color octet fermion.

Perhaps the "squark" is an ordinary color triplet scalar.

Example: models of weak-scale supersymmetry and universal extra dimensions (UED) with $R^{-1} \sim 1$ TeV both possess a spectrum of new particles (both colored and uncolored) that are accessible to the LHC.*
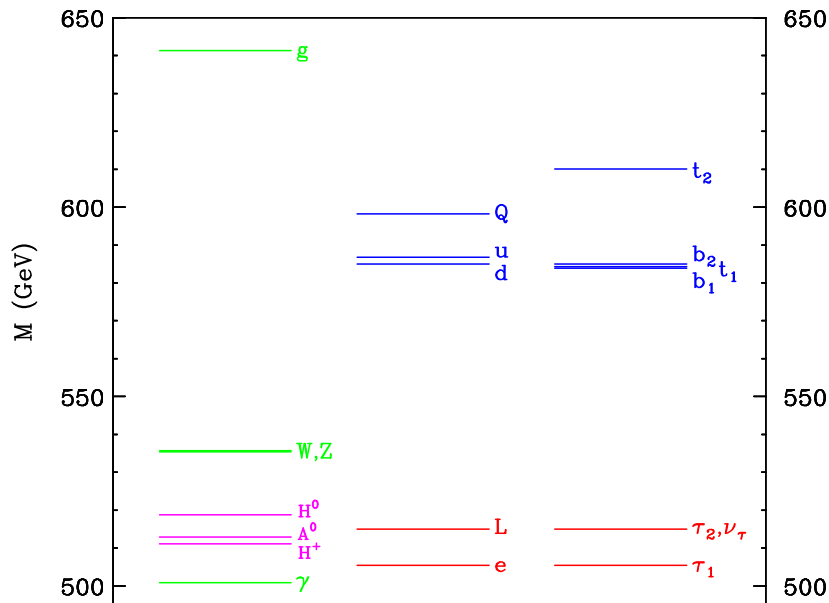
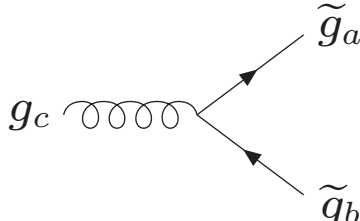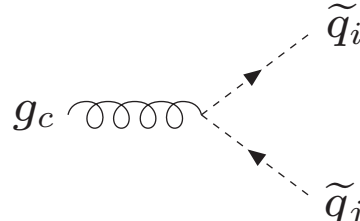first KK level in minimal UED
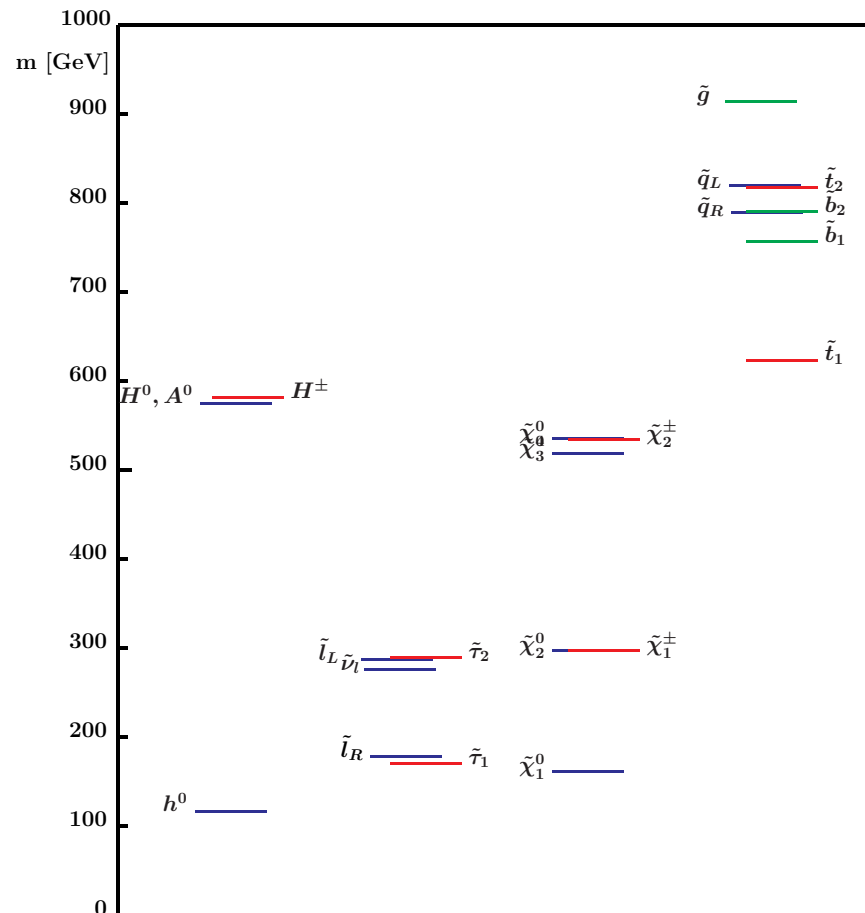
mSUGRA benchmark "SPS 3"

*For techniques to discriminate between these models, see e.g., A. Datta, K. Kong and K.T. Matchev, Phys. Rev. **D72**, 096006 (2005); J. M. Smillie and B.R. Webber, JHEP **0510**, 069 (2005).

A smoking gun for SUSY—Yukawa couplings related to gauge couplings

Example: gluino and squark couplings
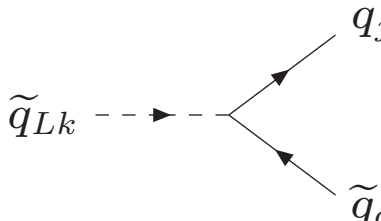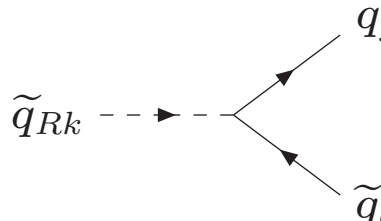
These vertices are governed solely by QCD. In contrast, the $\widetilde{q}q\widetilde{g}$ coupling is a scalar–scalar-fermion (Yukawa) coupling. In general, Yukawa and gauge interactions are unrelated. But, here it is the underlying supersymmetry that relates them.

The Yukawa couplings are proportional to the gauge coupling g_s. This is a smoking gun for supersymmetry.

SUSY coupling relations

In a supersymmetric field theory, the tree-level supersymmetric gaugino–fermion–sfermion interactions originate from the Kähler term:

$$\mathcal{L}_K = \int d^4\theta\, \Phi_i^\dagger (e^{2gV})_{ij}\Phi_j \ni i\sqrt{2}g_a(\varphi_i^* T_{ij}^a \psi_j \lambda^a - \bar{\lambda}^a \bar{\psi}_i T_{ij}^a \varphi_j)\,,$$

where $V = (A_\mu^a, \lambda^a, D^a)$ is a gauge vector superfield and the superfields $\Phi_i = (\varphi_i, \psi_i, F_i)$ include the Higgs, quark and lepton superfields. Thus, the gaugino–fermion–sfermion Yukawa couplings are related to gauge couplings.

Likewise, the tree-level higgsino–fermion–sfermion interactions originate from the superpotential:

$$\mathcal{L}_W = \int d^2\theta\, W(\Phi) + \text{h.c.} \ni -\tfrac{1}{2}\sum_{i,j} \frac{d^2 W(\varphi)}{d\varphi_i d\varphi_j}\left[\psi_i\psi_j + \text{h.c.}\right],$$

where $W(\Phi) \ni h_{ijk}\Phi_i\Phi_j\Phi_k$. This relates the Higgs–fermion–fermion and higgsino–fermion–sfermion couplings to h_{ijk}.

Testing SUSY coupling relations at colliders

To verify coupling relations requires a precision SUSY program. This is *not* a program for early LHC running.

Let us imagine that after years of LHC running, a spectrum of new particles is discovered, which is suggestive of SUSY. We wish to experimentally confirm the SUSY interpretation by verifying the SUSY coupling relations. This is a program for the high-luminosity running of the LHC and the ILC/CLIC in the following decade.

At the LHC, one might first try to verify the relation of the $\widetilde{q}q\widetilde{g}$ coupling to the strong gauge coupling. A study by Freitas, Skands, Spria and Zerwas [JHEP **0707**, 025 (2007)] demonstrated the feasibility of this measurement, although with some SUSY model dependence and reliance on ILC data.

Instead, we propose to go after the SUSY coupling relations involving the lightest supersymmetric particle (LSP), assumed to be the $\widetilde{\chi}_1^0$.

Expectations for the LSP

We assume R-parity-conserving SUSY, in which case the LSP is stable. A natural candidate for the LSP is $\widetilde{\chi}_1^0$. In general,

$$\widetilde{\chi}_1^0 = N_{11}\widetilde{B} + N_{12}\widetilde{W}^3 + N_{13}\widetilde{H}_d^0 + N_{14}\widetilde{H}_u^0.$$

The neutralino mass matrix is governed by gaugino mass parameters M_1 and M_2 and a supersymmetric higgsino mass parameter μ.

1. mSUGRA models typically give $m_Z \lesssim |M_1| \simeq \frac{1}{2}|M_2| \ll |\mu|$, which yields

$$\implies \quad \widetilde{\chi}_1^0 \simeq \widetilde{B} \text{ (the bino)}$$

2. In anomaly mediation, $M_i \simeq \dfrac{b_i g_i^2}{16\pi^2} m_{3/2}$, where $m_{3/2}$ is the gravitino mass and the b_i are the coefficients of the MSSM gauge beta-functions corresponding to the corresponding U(1), SU(2), and SU(3) gauge groups: $(b_1, b_2, b_3) = (\frac{33}{5}, 1, -3)$. Hence, $M_1 \simeq 2.8 M_2$. Assuming $M_2 \ll |\mu|$, then

$$\implies \quad \widetilde{\chi}_1^0 \simeq \widetilde{W}^3 \text{ (the neutral wino)}$$

In this case, $\{\widetilde{\chi}_1^0, \widetilde{\chi}_1^\pm\}$ comprise a nearly mass-degenerate SU(2)$_L$ triplet.

The neutralino mass matrix

Defining the two-component fermion fields, $\psi = (-i\lambda', -i\lambda^3, \psi_{H_d}^1, \psi_{H_u}^2)$,

$$\mathcal{L}_{\mathrm{mass}} = -\tfrac{1}{2}\psi_i(\mathcal{M}_N)_{ij}\psi_j + \text{h.c.},$$

where

$$\mathcal{M}_N = \begin{pmatrix} M_1 & 0 & -g'v_d/\sqrt{2} & g'v_u/\sqrt{2} \\ 0 & M_2 & gv_d/\sqrt{2} & -gv_u/\sqrt{2} \\ -g'v_d/\sqrt{2} & gv_d/\sqrt{2} & 0 & -\mu \\ g'v_u/\sqrt{2} & -gv_u/\sqrt{2} & -\mu & 0 \end{pmatrix}.$$

The physical neutralino masses are identified by:

$$N^* \mathcal{M}_N N^{-1} = \mathrm{diag}(m_{\tilde{\chi}1}, m_{\tilde{\chi}2}, m_{\tilde{\chi}3}, m_{\tilde{\chi}4}).$$

In the limit where M_1, M_2, and μ are larger than m_Z, then the mass eigenstates are approximately $\widetilde{B}$ (bino), $\widetilde{W}^3$ (neutral wino), $\widetilde{H}_d^0$ and $\widetilde{H}_u^0$ (neutral higgsinos), with corresponding masses $\sim |M_1|$, $|M_2|$, $|\mu|$ and $|\mu|$.

One cannot rule the other possibilities, which are less common in the literature:

3. Models in which $m_Z \lesssim |\mu| \ll M_1, M_2$.
$$\implies \quad \widetilde{\chi}_1^0 \simeq \widetilde{H} \text{ (the higgsino)}$$

4. Models in which there is significant mixing among gauginos and higgsinos in the $\widetilde{\chi}_1^0$ wave function.

We adopt a strategy that focuses on the possibility that $\widetilde{\chi}_1^0$ is nearly pure bino or pure wino. Ultimately, analyses of the type that will be presented here can be used to confirm or rule out such an assumption.

Note: If $\widetilde{\chi}_1^0$ is a major component of the dark matter, then identifying its gaugino and higgsino content will be especially important. Determining the content of the LSP will be a byproduct of our analysis.

A proposal to measure the $\widetilde{q}q\widetilde{\chi}_1^0$ coupling using monojet events at the LHC

The production process process involves the $\widetilde{q}q\widetilde{\chi}_1^0$ coupling, λ. If the $\widetilde{\chi}_1^0$ is dominantly gaugino-like, then this coupling is directly related to the gauge coupling due to SUSY.
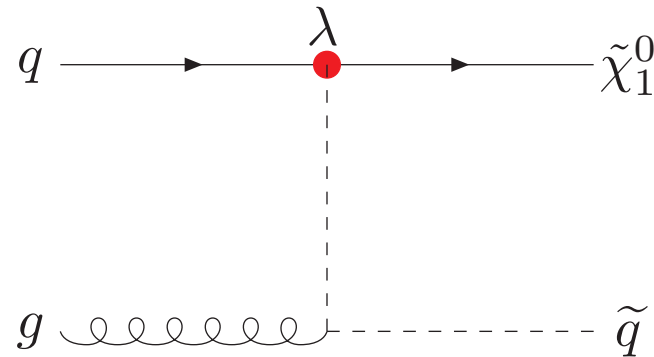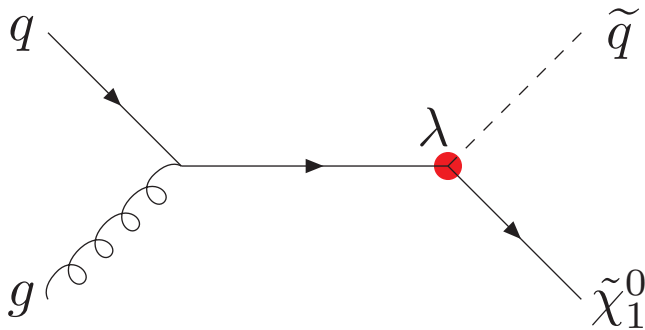
If the squark is lighter than the gluino, the squark will often decay directly to the LSP, resulting in a quark jet plus missing energy, i.e. a monojet event.
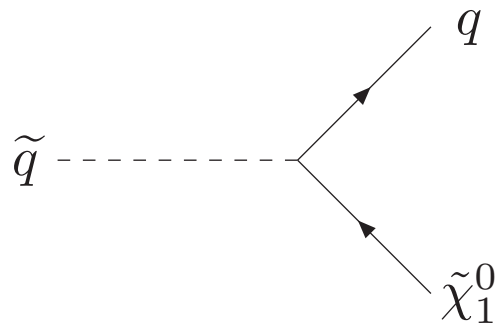
The Jacobian peak in the p_T distribution

Consider the $2 \rightarrow 3$ partonic scattering process,

$$q + g \rightarrow \widetilde{q} + \widetilde{\chi}_1^0 \,, \quad \text{followed by} \;\; \widetilde{q} \rightarrow q + \widetilde{\chi}_1^0 \,,$$

The quarks and gluon are treated as massless. The squark and neutralino masses are denoted by M and m, respectively. In the center-of-mass frame, the four-momenta of the initial quark and gluon and the final state quark jet are denoted by p_a, p_b and p_1, where

$$p_a = \tfrac{1}{2}\sqrt{s}\,(1\,;\,0\,,\,0\,,\,1)\,, \qquad p_b = \tfrac{1}{2}\sqrt{s}\,(1\,;\,0\,,\,0\,,\,-1)\,,$$

$$p_1 = E_1(1\,;\,\sin\theta\,,\,0\,,\,\cos\theta)\,,$$

and $\sqrt{s}$ is the partonic center-of-mass energy. The transverse momentum of the final state quark jet is $p_T = E_1 \sin\theta$. The kinematical limits of p_T and E_1 are:

$$\text{for } 0 \le p_T \le E_1^- \,, \qquad E_1^- \le E_1 \le E_1^+ \,,$$

$$\text{for } E_1^- \le p_T \le E_1^+ \,, \qquad p_T \le E_1 \le E_1^+ \,,$$

where

$$E_1^{\pm} \equiv \frac{M^2 - m^2}{4M^2\sqrt{s}}\left[s + M^2 - m^2 \pm \sqrt{(s + M^2 - m^2)^2 - 4sM^2}\right] \,.$$

We will also make use of the kinematic invariants,

$$t_1 \equiv (p_a - p_1)^2 = -\sqrt{s}\left[E_1 - \sqrt{E_1^2 - p_T^2}\right], \qquad s_2 \equiv (p_a + p_b - p_1)^2 = s - 2\sqrt{s}E_1.$$

The p_T distribution of the quark jet is then given by:

$$\frac{d\sigma}{dp_T} = \frac{Bp_T}{8\pi\xi s^{3/2}} \int_{E_{\min}}^{E_{\max}} \frac{dE_1}{E_1\sqrt{E_1^2 - p_T^2}} |C_1(s, t_1)|^2$$

where $\xi \equiv 1 - m^2/M^2$, C_1 is the matrix element for $qg \to \widetilde{q}\widetilde{\chi}_1^0$, $B \equiv \mathrm{BR}(\widetilde{q} \to q\widetilde{\chi}_1^0)$ and the limits of integration are given by $E_{\max} \equiv E_1^+$ and

$$E_{\min} = \begin{cases} E_1^- & \text{for } 0 \le p_T \le E_1^-, \\ p_T & \text{for } E_1^- \le p_T \le E_1^+. \end{cases}$$

In obtaining the above result, we made use of $dt_1 ds_2 = s(E_1^2 - p_T^2)^{-1/2} dp_T^2 dE_1$. This Jacobian factor is responsible for the peak in the p_T distribution at:
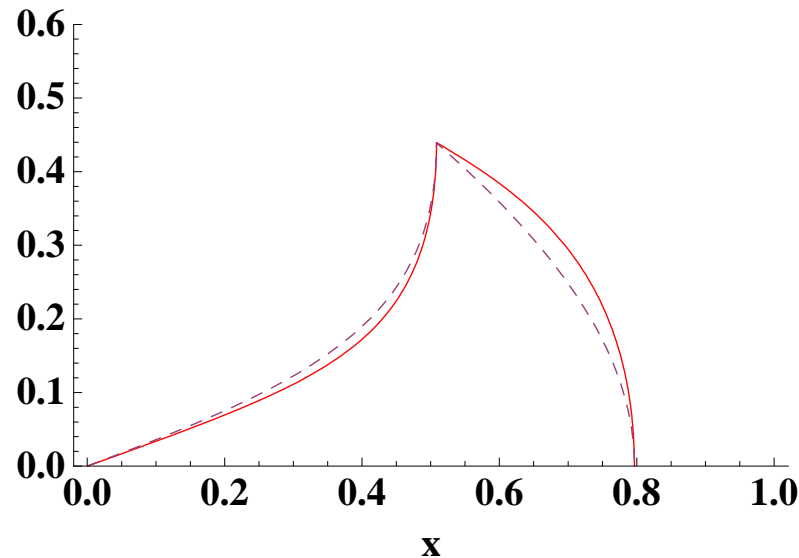
$$(p_T)_{\mathrm{peak}} = E_1^- = \frac{\xi}{4\sqrt{s}}\left[s + M^2 - m^2 - \sqrt{(s + M^2 - m^2)^2 - 4sM^2}\right]$$

which arises at the boundary where $E_{\min}$ switches from E_1^- to p_T.

For $C_1 = 1$ (pure phase space), the integral over E_1 can be carried out explicitly,

$$\frac{d\sigma}{dp_T} = \frac{B}{8\pi\xi s^{3/2}} \left[\tan^{-1}\left(\frac{\sqrt{[E_1^+]^2 - p_T^2}}{p_T} \right) - \Theta(E_1^- - p_T)\tan^{-1}\left(\frac{\sqrt{[E_1^-]^2 - p_T^2}}{p_T} \right) \right].$$

Employing the actual $qg \to \widetilde{q}\widetilde{\chi}_1^0$ matrix element yields only a small correction to the shape of the p_T distribution. Note that $(p_T)_{\max} = E_1^+$, so that $x_{\max} = 2(p_T)_{\max}/\sqrt{s} < 1$.

Unnormalized cross-section as a function of $x \equiv 2p_T/\sqrt{s}$ for $qg \to \widetilde{q}\widetilde{\chi}_1^0 \to q\widetilde{\chi}_1^0\widetilde{\chi}_1^0$, (solid curve), assuming $M_{\widetilde{q}}^2 = 0.5s$ and $m_{\widetilde{\chi}}^2 = 0.05s$. If the matrix element for $qg \to \widetilde{q}\widetilde{\chi}_1^0$ is set equal to unity, one obtains the dashed curve. The relative normalization of the two curves has been fixed such that the height of the peaks of the distributions coincide.

The location of the Jacobian peak depends on the partonic center-of-mass energy. But, when computing the p_T distribution of $pp \rightarrow \widetilde{q}\widetilde{\chi}_1^0 \rightarrow q\widetilde{\chi}_1^0\widetilde{\chi}_1^0$, one must integrate over the parton distribution functions. In the convolution, partonic center-of-mass energies close to the energy threshold for the partonic process provide the dominant contribution to the production of the final state. The threshold corresponds to $\sqrt{s} = M + m$, which yields

$$E_1^- = E_1^+ = \frac{M^2 - m^2}{2M}.$$

Thus, close to threshold,

$$(p_T)_{\text{peak}} = E_1^- \simeq \frac{M^2 - m^2}{2M} = \tfrac{1}{2}\xi M,$$

which is independent of the partonic center-of-mass energy.

As $\sqrt{s}$ is increased above the threshold energy, the value of E_1^- *decreases* relative to the above estimate. Thus, we expect the actual peak in the transverse momentum distribution of the hadronic scattering process (or equivalently in the missing transverse energy distribution) to be somewhat less than the above result.

The signal processes—further details

- For a bino LSP: $g + u \to \tilde{\chi}_1^0 + \tilde{u}_R$, $g + d \to \tilde{\chi}_1^0 + \tilde{d}_R$ followed by $\tilde{u}_R \to u\tilde{\chi}_1^0$ or $\tilde{d}_R \to d\tilde{\chi}_1^0$. The charge-conjugated processes are also included. Here, $\lambda = g'$, the $U(1)_Y$ gauge coupling.

  - Since $\tilde{q}_R$ is an $SU(2)_L$-singlet, $\mathrm{BR}(\tilde{q}_R \to q\tilde{\chi}_1^0) \simeq 100\%$.

- For a wino LSP: $g + u \to \tilde{\chi}_1^0 + \tilde{u}_L$, $g + d \to \tilde{\chi}_1^0 + \tilde{d}_L$, $g + u \to \tilde{\chi}_1^+ + \tilde{d}_L$, $g + d \to \tilde{\chi}_1^- + \tilde{u}_L$, where $\tilde{u}_L \to u\tilde{\chi}_1^0/d\tilde{\chi}_1^+$, $\tilde{d}_L \to d\tilde{\chi}_1^0/u\tilde{\chi}_1^-$ and $\tilde{\chi}_1^+ \to S + \tilde{\chi}_1^0$, where S is either a very soft lepton or QCD radiation too soft to be identified as a jet. The charge-conjugated processes are also included. Here, $\lambda = g$, the $SU(2)_L$ gauge coupling.

  - The mass splitting between $\tilde{\chi}_1^+$ and $\tilde{\chi}_1^0$ is ~ 200 MeV, so the dominant decay $\tilde{\chi}_1^+ \to \tilde{\chi}_1^0 \pi^+$ typically results in an unmeasurable soft pion.
  - Since $\tilde{q}_L$ is an $SU(2)_L$-triplet, there is a preference for the direct decay of $\tilde{q}_L \to q\tilde{\chi}_1^0$.

Significant SM and SUSY backgrounds

- $Z(\to \nu\bar{\nu})$+jet. This background can be ascertained from the $Z(\to \ell^+\ell^-)$+jet signal. In principle, this background can be subtracted off from the monojet sample.

- $W(\to \tau\nu)$+jet, where the W decays into a tau and a neutrino, and the tau is either not detected, or lost in the jet.

- $W(\to e/\mu\,\nu)$+jet, where the W decays into an electron or a muon and a neutrino and the electron/muon is undetected or lost inside the jet.

- QCD jet production with mismeasurement of the energy deposited in the detector. One could produce di-jets, for instance, and one of the jets could be lost in the detector (or its energy mismeasured so that it fluctuate below the transverse momentum required to identify the jet).

- $\widetilde{q}\widetilde{q}$ production, where the decay products of the two squarks merge into a single jet.

- $\widetilde{\chi}^0_1\widetilde{\chi}^0_1$ production plus an initial state radiated (ISR) jet.

- In the case of a wino LSP, $\widetilde{\chi}^+_1\widetilde{\chi}^-_1$ production plus an ISR jet will yield monojet events, since $\widetilde{\chi}^+_1 \to \widetilde{\chi}^0_1 +$ soft pion.

Simulation of signal and backgrounds

The following tools have been employed:

- `Herwig++2.4.2`

  - signal and backgrounds at tree-level have been simulated
  - pair production and the two and three body decay of all SUSY particles included

- `Herwig++` output analyzed using `HepMC-2.04.02` and `ROOT`

- Jets were reconstructed using `fastjet-2.4.1`

  - Jets are defined with $p_T > 30$ GeV, and the anti-k_t jet algorithm with $R \equiv \sqrt{(\Delta\eta)^2 + (\Delta\phi)^2} = 0.7$ was used.

- SUSY spectrum determined with `SOFTSUSY3.0.13` and applied to a benchmark bino-LSP and wino-LSP scenarios

Wino-LSP case study

We examine the benchmark mAMSB scenario with:

$$M_{3/2} = 33\,\text{TeV}, \ \ M_0 = 200\,\text{GeV}, \ \tan\beta = 10, \ \text{sgn}(\mu) = +1\,,$$

which gives $\sigma(pp \to \widetilde{q}_R \widetilde{\chi}_1^0) = 470$ fb, $\lambda = 0.99g$ and the following SUSY spectrum:

sparticle	mass [GeV]	sparticle	mass [GeV]
$\widetilde{\chi}_1^0$	106.5	$\widetilde{\chi}_4^0$	593
$\widetilde{\chi}_1^+$	106.7	$\widetilde{\chi}_2^+$	594
$\widetilde{\tau}_1$	113	$\widetilde{b}_1$	634
$\widetilde{\nu}_\tau$	135	$\widetilde{t}_2$	688
$\widetilde{\nu}_e/\widetilde{\nu}_\mu$	138	$\widetilde{u}_L/\widetilde{c}_L$	722
$\widetilde{e}_R/\widetilde{\mu}_R$	150	$\widetilde{b}_2$	723
$\widetilde{e}_L/\widetilde{\mu}_L$	159	$\widetilde{d}_L/\widetilde{s}_L$	726
$\widetilde{\tau}_2$	179	$\widetilde{u}_R/\widetilde{c}_R$	726
$\widetilde{\chi}_2^0$	298	$\widetilde{d}_R/\widetilde{s}_R$	732
$\widetilde{t}_1$	521	$\widetilde{g}$	745
$\widetilde{\chi}_3^0$	584		

The cuts employed in our analysis are summarized below, based on an integrated luminosity of 100 fb^{-1} at $\sqrt{s} = 14$ TeV.

cut	all SM	SUSY bkg.	signal	$S/\sqrt{B}$ ($S/\sqrt{7B}$)
$p_T(\text{jet1})$, $\not{p}_T > 100$ GeV	3.81×10^7	1.04×10^6	44 100	-
lepton veto	2.52×10^7	621 000	43 800	-
$p_T(\text{jet2}) < 50$ GeV	1.73×10^7	111 000	16 200	3.9 (1.5)
$\not{p}_T > 300$ GeV	171 000	11 000	8 390	20 (7.7)
$m(\text{jet1}) < 80$ GeV	135 000	6 020	6 370	17 (6.5)
tau veto	119 000	5 840	6 370	18 (7.0)
b-jet veto	115 000	5 290	6 320	19 (7.0)

The lepton veto removes events with an isolated electron or muon with $p_T > 5$ GeV and $|\eta| < 2.5$. The isolation criterion demands ≤ 10 GeV of additional energy in a cone of radius $\Delta R = 0.2$. The conservative statistical estimator $S/\sqrt{7B}$ should be used (according to L. Vacavant and I. Hinchliffe) if statistical fluctuations are dominated by the $Z(\rightarrow \ell^+\ell^-) + \text{jet}$ calibration sample used to subtract the $Z(\rightarrow \nu\bar{\nu}) + \text{jet}$ background.

Note that we need a good signal to SUSY background if we wish to measure the $\tilde{q}q\tilde{\chi}_1^0$ coupling λ to good precision. This is the main reason for the cut on $m(\text{jet1})$. The τ and b-jet vetoes are not used in our final analysis.
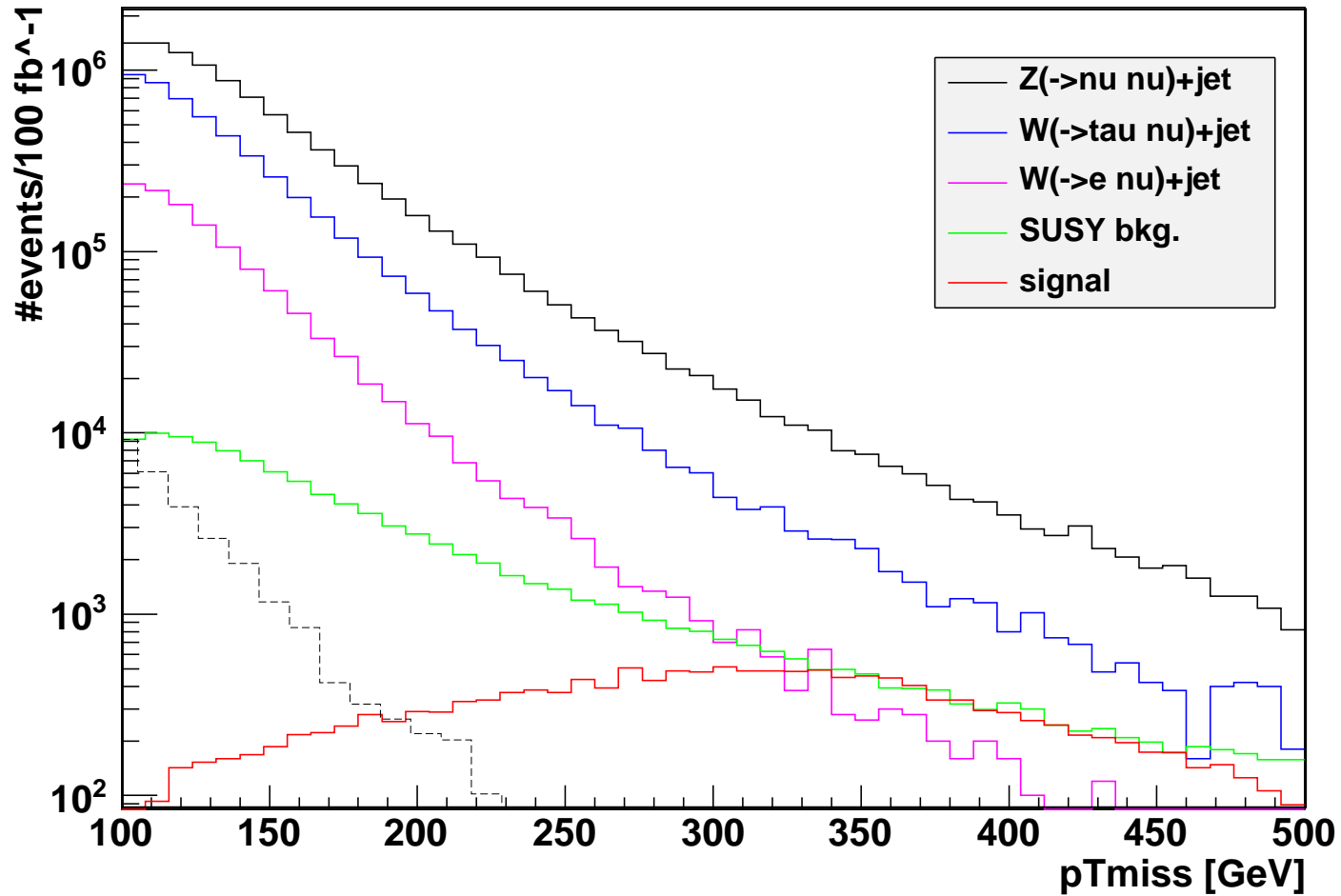
The QCD background is shown as a black dashed histogram. The first three cuts listed in the previous table have been applied. The signal exhibits a Jacobian peak, whose position depends on the $\widetilde{q}$ and $\widetilde{\chi}_1^0$ masses.
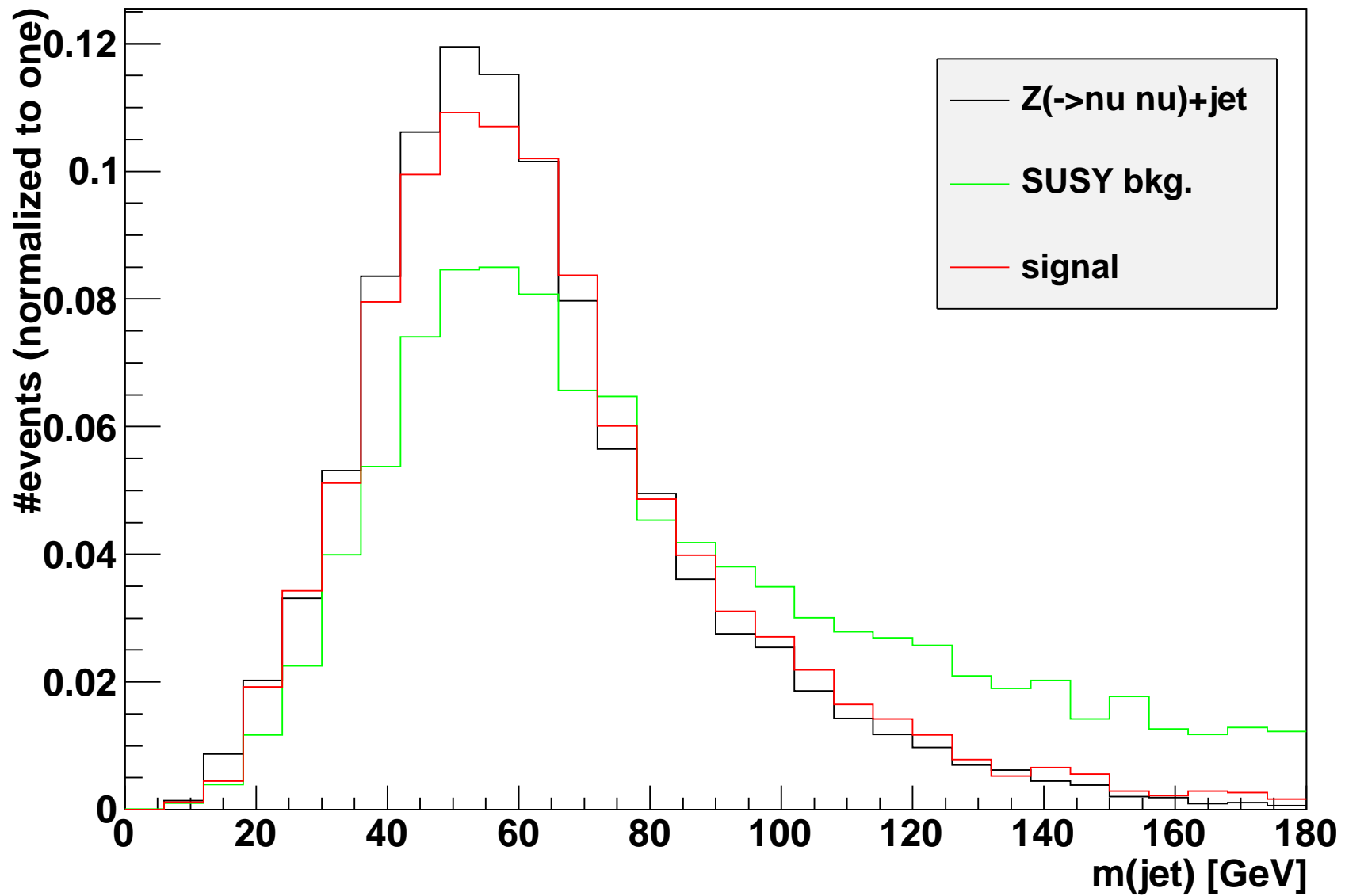
The invariant mass distribution of the hardest jet, normalized to one. The first four cuts listed in the previous table have been applied. The QCD background has a distribution almost indistinguishable from that of $Z(\to \nu\bar{\nu}) + \mathrm{jet}$.

Accuracy in the determination of the $\widetilde{q}q\widetilde{\chi}_1^0$ coupling λ in the wino case study

error	$\Delta\sigma_{\mathrm{mono}}/\sigma_{\mathrm{mono}}$	$\Delta\lambda/\lambda$
luminosity	3%	1.5%
PDF uncertainty	17%	8.3%
NLO corrections	18%	9%
sparticle mass $\Delta\tilde{m} = 10$ GeV	7.3%	3.7%
statistics (optimistic)	5.8%	2.9%
statistics (conservative)	15%	7.7%
total (optimistic)	26%	13%
total (conservative)	30%	15%

Relative errors for the signal monojet cross section (second column) and the $\widetilde{q}_L q\widetilde{\chi}_1^0$ coupling (third column) from different sources (first column). The numbers are for the mAMSB benchmark scenario.

An optimal choice of cuts depends on the squark and neutralino mass. We search in steps of 10 GeV for the p_T and $m(\text{jet1})$ cuts that provide the highest $S/\sqrt{S+B}$. The best significance is near the Jacobian peak. Applying these optimal cuts yields:
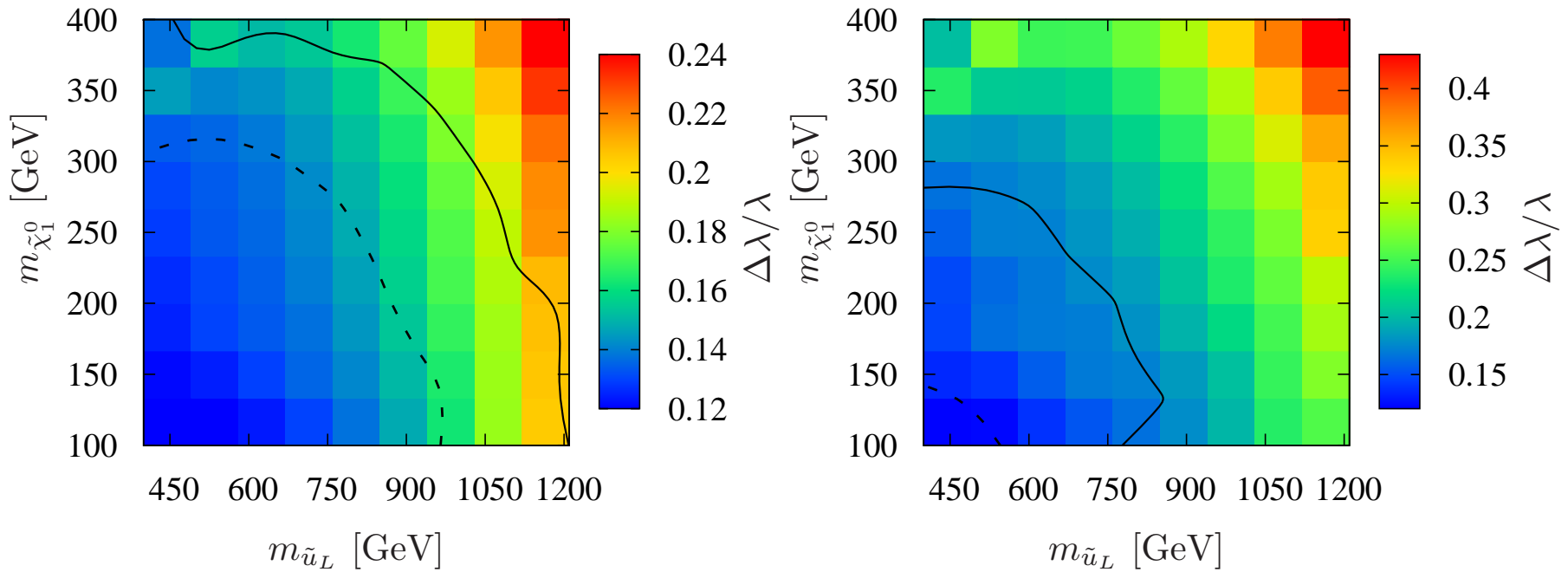
Fractional precision to which the $\widetilde{q}_L q \widetilde{\chi}_1^0$ coupling λ can be reconstructed as function of the squark and $\widetilde{\chi}_1^0$ mass. The left (right) figure employs our optimistic (conservative) estimate for the SM background uncertainties. The solid and dashed black lines correspond to $S/\sqrt{B}$ ($S/\sqrt{7B}$) of 5σ and 10σ, respectively.

Bino-LSP case study

We examine a benchmark light mSUGRA scenario for the bino-LSP case study with:

$$M_0 = 220\,\mathrm{GeV},\ M_{1/2} = 180\,\mathrm{GeV},\ A_0 = -500\,\mathrm{GeV},\ \tan\beta = 20,\ \mathrm{sgn}(\mu) = +1\,,$$

which gives $\sigma(pp \rightarrow \tilde{q}_R \tilde{\chi}_1^0) = 520$ fb, $\lambda = 0.99g'$ and the following SUSY spectrum:

sparticle	mass [GeV]	sparticle	mass [GeV]
$\tilde{\chi}_1^0$	70.2	$\tilde{\chi}_4^0$	365
$\tilde{\chi}_1^+$	132	$\tilde{\chi}_2^+$	370
$\tilde{\chi}_2^0$	133	$\tilde{b}_1$	378
$\tilde{\tau}_1$	189	$\tilde{b}_2$	443
$\tilde{t}_1$	226	$\tilde{u}_R/\tilde{c}_R$	454
$\tilde{\nu}_\tau$	230	$\tilde{d}_R/\tilde{s}_R$	455
$\tilde{e}_R/\tilde{\mu}_R$	234	$\tilde{g}$	456
$\tilde{\nu}_e/\tilde{\nu}_\mu$	242	$\tilde{u}_L/\tilde{c}_L$	463
$\tilde{e}_L/\tilde{\mu}_L$	255	$\tilde{d}_L/\tilde{s}_L$	470
$\tilde{\tau}_2$	259	$\tilde{t}_2$	477
$\tilde{\chi}_3^0$	359		

Accuracy in the determination of the $\widetilde{q}q\widetilde{\chi}_1^0$ coupling λ in the bino case study

error	$\Delta\sigma_{\mathrm{mono}}/\sigma_{\mathrm{mono}}$	$\Delta\lambda/\lambda$
luminosity	3.0%	1.5%
PDF uncertainty	17%	8.3%
NLO corrections	16%	8.0%
sparticle mass $\Delta\widetilde{m} = 10$ GeV	11%	5.6%
statistics (optimistic)	8.6%	4.3%
statistics (conservative)	23%	11%
total (optimistic)	27%	14%
total (conservative)	35%	17%

Relative errors for the signal monojet cross section (second column) and the $\widetilde{\chi}_1^0\widetilde{q}_Rq$ coupling λ (third column) from different sources (first column). The numbers are for the light mSUGRA benchmark scenario. In isolating the signal, the second jet veto is now tighter, with $p_T(\mathrm{jet2}) < 30$ GeV. The $\not{p}_T$ cut is lowered to 180 GeV and the $m(\mathrm{jet1})$ cut is lowered to 70 GeV to optimize for the lighter SUSY spectrum.

Summary of the Wino-LSP and Bino-LSP case studies

- For a wino-LSP, one can test the $\widetilde{q}q\widetilde{\chi}_1^0$ coupling relation to a precision of $\sim 10\%$—20% at the LHC with $\sqrt{s} = 14$ TeV and 100 fb^{-1} of data if squark masses are below 1 TeV, over a significant portion of the wino-LSP parameter space.

- For a bino-LSP, precisions of $\sim 10\%$—20% are achievable if squark masses are below 500 GeV and the LSP mass is below 100 GeV.

The more favorable results for the wino-LSP are a consequence of a significantly larger $\sigma(qg \rightarrow \widetilde{q}\widetilde{\chi}_1^0)$, which follows from the fact that $g^2/g'^2 \simeq 3$. This means that it should also be possible to employ the monojet signal to distinguish between a wino, bino and higgsino LSP. In the case of a higgsino LSP, $qg \rightarrow \widetilde{q}\widetilde{\chi}_1^0$ is highly suppressed and no corresponding contribution to the monojet signal will be observed.

Precision studies of SUSY coupling relations

Recall that the tree-level supersymmetric gaugino–fermion–sfermion interactions originate from the Kähler term:

$$\mathcal{L}_K = \int d^4\theta \, \Phi_i^\dagger (e^{2gV})_{ij} \Phi_j \ni i\sqrt{2} g_a (\phi_i^* T_{ij}^a \psi_j \lambda^a - \bar{\lambda}^a \bar{\psi}_i T_{ij}^a \phi_j) \,.$$

Let us examine all possible dimension-four gauge-invariant operators in the gaugino–higgsino–Higgs boson sector that violate supersymmetry. One class of operators includes:

$$\frac{ig_u}{\sqrt{2}} \lambda^a \tau_{ij}^a \psi_{H_u}^j H_u^{*i} + \frac{ig_d}{\sqrt{2}} \lambda^a \tau_{ij}^a \psi_{H_d}^j H_d^{*i} + \frac{ig_u'}{\sqrt{2}} \lambda' \psi_{H_u}^i H_u^{*i} - \frac{ig_d'}{\sqrt{2}} \lambda' \psi_{H_d}^i H_d^{*i} + \text{h.c.} \,,$$

where the coupling g_u, g_d, g_u' and g_d' deviate from their supersymmetric values given by the SU(2) and U(1)$_Y$ gauge couplings, g and g', respectively. Such effects are generated by one-loop corrections and have been studied in detail by Katz et al. and by Kiyoura et al.

Wrong Higgs gaugino–higgsino operators

Here, we focus on a second class of supersymmetric violating operators:

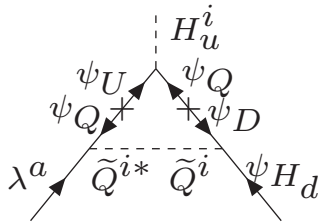$$ig k_1 \lambda^a \tau^a_{ij} \psi^j_{H_u} \epsilon_{ki} H^k_d \,, \qquad\qquad ig' k_2 \lambda' \psi^k_{H_u} \epsilon_{ki} H^i_d \,,$$

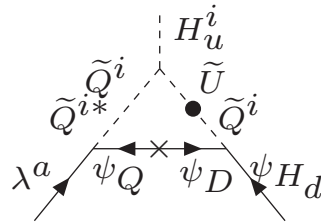$$ig k_3 \lambda^a \tau^a_{ij} \psi^j_{H_d} \epsilon_{ki} H^k_u \,, \qquad\qquad ig' k_4 \lambda' \psi^i_{H_d} \epsilon_{ki} H^k_u \,.$$

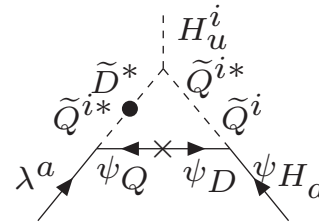## Integrating out a subset of heavy MSSM fields

Graphs (a), (b) and graph (c) are suppressed by $\mathcal{O}(m_t m_b / M^2_{\mathrm{SUSY}})$ and $\mathcal{O}(m^2_b / M^2_{\tilde{q}})$, respectively, and hence decouple when $M_{\tilde{q}} \gg M_{\tilde{\chi}}, M_H, m_Z$.

(a)   (b)   (c)

One-loop diagrams contributing to the wrong-Higgs gaugino operators. The cross ($\times$) indicates the two-component fermion propagator that is proportional to the corresponding Dirac mass. In (b) and (c) the solid dot indicates an insertion of the Higgs vacuum expectation value (vev). Field labels correspond to annihilation at each vertex of the triangle. Replacing the Higgs vev by the appropriate Higgs field, these diagrams actually correspond to dimension-six operators with the expected decoupling behavior.

Implications for chargino observables

After the neutral Higgs bosons acquire their vacuum expectation values, $\langle H_u^0 \rangle = v_u/\sqrt{2}$ and $\langle H_d^0 \rangle = v_d/\sqrt{2}$, the quadratic terms of the effective gaugino Lagrangian are given by:

$$\mathcal{L}_{\text{mass}} = \frac{ig_u v_u}{2}\lambda^a \tau_{2j}^a \psi_{H_u}^j + \frac{ig_d v_d}{2}\lambda^a \tau_{1j}^a \psi_{H_d}^j + \frac{ig_u' v_u}{2}\lambda' \psi_{H_u}^2 - \frac{ig_d' v_d}{2}\lambda' \psi_{H_d}^1$$

$$- M\lambda^a \lambda^a - M'\lambda'\lambda' - \mu\epsilon_{ij}\psi_{H_u}^i \psi_{H_d}^j + \frac{ik_1 v_d}{\sqrt{2}}\lambda^a \tau_{2j}^a \psi_{H_u}^j$$

$$- \frac{ik_2 v_d}{\sqrt{2}}\lambda' \psi_{H_u}^2 - \frac{ik_3 v_u}{\sqrt{2}}\lambda^a \tau_{1j}^a \psi_{H_d}^j - \frac{ik_4 v_u}{\sqrt{2}}\lambda' \psi_{H_d}^1 + \text{h.c.}$$

The parameters appearing above are effective parameters below the TeV-scale. For example, $g_u = g + \delta g_u$, $g_d = g + \delta g_d$, $g_u' = g' + \delta g_u'$, and $g_d' = g' + \delta g_d'$, where the $\delta g's$ include threshold and renormalization group effects from SUSY breaking below the fundamental SUSY-breaking scale.

Isolating the terms that contribute to the chargino matrix, we introduce

$$\psi_i^+ = \begin{pmatrix} -i\lambda^+ \\ \psi_{H_u}^1 \end{pmatrix}, \qquad \psi_i^- = \begin{pmatrix} -i\lambda^- \\ \psi_{H_d}^2 \end{pmatrix},$$

where $\lambda^\pm = \frac{1}{\sqrt{2}}(\lambda^1 \mp i\lambda^2)$. Then, the chargino mass terms are given by:

$$\mathcal{L}_{\text{mass}} = -\frac{1}{2} \begin{pmatrix} \psi^+ & \psi^- \end{pmatrix} \begin{pmatrix} 0 & (X^{\text{eff}})^T \\ X^{\text{eff}} & 0 \end{pmatrix} \begin{pmatrix} \psi^+ \\ \psi^- \end{pmatrix} + \text{h.c.},$$

where

$$X^{\text{eff}} = \begin{pmatrix} M & (g + \delta g_u)\dfrac{v_u}{\sqrt{2}} \left(1 - \dfrac{\sqrt{2}k_1 \cot\beta}{g + \delta g_u} \right) \\ (g + \delta g_d)\dfrac{v_d}{\sqrt{2}} \left(1 + \dfrac{\sqrt{2}k_3 \tan\beta}{g + \delta g_d} \right) & \mu \end{pmatrix}$$

with $v_u \equiv v \sin\beta$ and $v_d \equiv v \cos\beta$.

We wish to identify the leading effect at large $\tan\beta$. We can neglect the effects of δg_d as these are one-loop effects with no $\tan\beta$-enhancements.

We shall write:

$$X_{12}^{\mathrm{eff}} = \sqrt{2}m_W \sin\beta \left(1 + \delta_{12}\right), \qquad X_{21}^{\mathrm{eff}} = \sqrt{2}m_W \cos\beta \left(1 + \delta_{21}\right).$$

In the large $\tan\beta$ limit, δ_{21} is $\tan\beta$-enhanced, and provides parametrically the largest of the one-loop corrections to X^{eff}.

$$\delta_{21} \simeq \frac{\sqrt{2}k_3 \tan\beta}{g}.$$

In the MSSM, k_3 is generically suppressed by a loop factor and a decoupling factor,

$$k_3 \sim \frac{g^2}{16\pi^2} \cdot \frac{m_Z^2}{M_{\tilde{q}}^2},$$

In models of gauge-mediated SUSY-breaking, additional loop contributions to the wrong-Higgs couplings from light messengers with $\mathcal{O}(1)$ couplings can enhance both suppression factors. The correction to the supersymmetric relation, $X_{21} = gv\cos\beta/\sqrt{2}$ can be as large as $\sim 50\%$ for $\tan\beta = 50$.

Given the effective chargino matrix X^{eff}, the chargino masses and mixing angles are obtained from:

$$U^* X V^{-1} = M_D \equiv \text{diag}(m_{\chi_1^+}, m_{\chi_2^+}) \,,$$

for some suitably chosen unitary matrices U and V, where the elements of the diagonal matrix M_D are real and non-negative.

Let Φ_μ be the relative phase between μ and M (and assume the phases of X_{12} and X_{21} are negligible). Then, the chargino squared-masses and mixing angles θ_L and θ_R are:[†]

$$m^2_{\chi_{1,2}^{\pm}} = \tfrac{1}{2}\left(M^2 + |\mu|^2 + X_{12}^2 + X_{21}^2 \mp \Delta\right) \,,$$

$$\cos 2\theta_{R,L} = \Delta^{-1}\left[|\mu|^2 - M^2 \pm (X_{12}^2 - X_{21}^2)\right] \,,$$

[†]One can also derive equations for the physical phases that appear in U and V, but these are not needed here.

where the quantity Δ is defined by:

$$\Delta \equiv \left[(M^2 - |\mu|^2 - X_{12}^2 + X_{21}^2)^2 + 4(M^2 X_{12}^2 + |\mu|^2 X_{21}^2 + 2M|\mu|X_{12}X_{21}\cos\Phi_\mu)\right]^{1/2}.$$

Taking δ_{12} and δ_{21} small, and working to first order in these quantities, one obtains two equations for the two unknown δ's. We find:

$$\delta_{21} = \frac{2s_\beta^2 f^{1/2}(\Delta - f^{1/2}) - \frac{1}{2}h\left\{c_{2\beta} + \frac{1}{4m_W^2}\left[(\cos 2\theta_R - \cos 2\theta_L)(m_{\chi_2^\pm}^2 - m_{\chi_1^\pm}^2)\right]\right\}}{hc_\beta^2 + gs_\beta^2},$$

where f, g and h are complicated (but known) expressions that depend on the two chargino masses, m_W, $\tan\beta$, $\cos 2\theta_{L,R}$, and $\cos\Phi_\mu$. These quantities can in principle be determined at the ILC using precision chargino data [cf. S.Y. Choi et al., EPJC 14 (2000) 535], using measurements of the total production cross-sections for $e^+e^- \to \widetilde{\chi}_i^\pm \widetilde{\chi}_j^\mp$ and asymmetries with polarized beams.

For the morbidly curious

It is convenient to define:

$$C_{RL}^{+} \equiv -(\cos 2\theta_R + \cos 2\theta_L)\,, \qquad\qquad C_{RL}^{-} \equiv \cos 2\theta_R - \cos 2\theta_L\,.$$

Then,

$$f = (\tfrac{1}{2}C_{RL}^{+}\Delta + 2m_W^2 c_{2\beta})^2 + 4m_W^2(m_{\chi_2^{\pm}}^2 + m_{\chi_1^{\pm}}^2 - 2m_W^2) - 2m_W^2 C_{RL}^{+}\Delta c_{2\beta}$$

$$+ 4m_W^2 \Gamma s_{2\beta}\cos\Phi\,,$$

$$g = 2m_W^2 c_\beta^2 \left[4(m_{\chi_2^{\pm}}^2 + m_{\chi_1^{\pm}}^2) + 4m_W^2 c_{2\beta} - 16m_W^2 - C_{RL}^{+}\Delta + 4\Gamma\tan\beta\cos\Phi \right.$$

$$\left. - \frac{8m_W^2}{\Gamma}(m_{\chi_2^{\pm}}^2 + m_{\chi_1^{\pm}}^2 - 2m_W^2)s_{2\beta}\cos\Phi \right]\,,$$

$$h = 2m_W^2 s_\beta^2 \left[4(m_{\chi_2^{\pm}}^2 + m_{\chi_1^{\pm}}^2) - 4m_W^2 c_{2\beta} - 16m_W^2 + C_{RL}^{+}\Delta + 4\Gamma\tan\beta\cos\Phi \right.$$

$$\left. - \frac{8m_W^2}{\Gamma}(m_{\chi_2^{\pm}}^2 + m_{\chi_1^{\pm}}^2 - 2m_W^2)s_{2\beta}\cos\Phi \right]\,,$$

where

$$\Gamma \equiv \left[(m_{\chi_1^{\pm}}^2 + m_{\chi_2^{\pm}}^2 - 2m_W^2)^2 - \tfrac{1}{4}(C_{RL}^{+}\Delta)^2 \right]^{1/2}\,.$$

Conclusions and future directions

- To confirm a SUSY interpretation of new physics, one must identify experimental observables that are sensitive to the underlying SUSY structure.

- The relation of gaugino–particle–sparticle couplings to gauge couplings is a smoking gun for SUSY.

- Monojet events at the LHC arising from $\widetilde{q}\widetilde{\chi}_1^0$ production can probe gaugino–quark–squark couplings with an accuracy approaching $\mathcal{O}(10\%)$ with 100 fb^{-1} of data at $\sqrt{s} = 14$ TeV over a significant portion of the MSSM parameter space, and can provide evidence in favor of a wino-like or bino-like LSP.

- In the future, we will examine multiple SUSY observables that are sensitive to the gaugino–particle–sparticle coupling. A global fit to these observables can enhance the precision of the coupling determinations, while providing stronger evidence in favor of the underlying SUSY structure.

- Ultimately, a precision program for SUSY requires an ILC and/or CLIC. Precision measurements of gaugino–particle–sparticle couplings can reveal deviations from the tree-level SUSY predictions, which can provide critical clues to the fundamental nature of SUSY-breaking.